

Isothermal Homogeneous Two-Phase Flow in Horizontal Pipes

C. T. HUEY and R. A. A. BRYANT

University of New South Wales, Sydney, Australia

In the first part of this paper a theory for isothermal homogeneous two-phase, liquid-gas flow in horizontal pipes is established by introducing the concept of Mach number and by considering the medium to be a pseudo gas. The theory takes account of wall friction, compressibility and flow choking. A set of working formulas is obtained. In the second part, results of experiments on homogeneous bubbly flows of water-air mixtures in a 1-in. pipe are reported. Criteria for the occurrence of bubbly flow are established and the occurrence of flow choking confirmed. It is shown that the mathematical model is adequate insofar as it explains, phenomenologically, real flow conditions.

PART I. THEORETICAL ANALYSIS

The object of this paper is to establish a simple mathematical model for flow in horizontal pipes of the homogeneous liquid-gas mixture known as bubbly flow or froth flow.

Some information on homogeneous liquid-gas mixtures is already available. It is known that this mixture has a low sound speed. Detailed studies of the propagation of shock waves through it and its flow behavior in convergent-divergent nozzles have already appeared in the literature (1 to 4). However there is little information on bubbly flow in pipes (5, 6).

In this paper it is shown that by considering the mixture to be a pseudo gas and by adopting an approach similar to the well-known Fanno line analysis of gas dynamics, it is possible to construct a mathematical model which will explain known flow properties of the medium. In particular the model accounts for the compressibility of the medium, for flow choking, and for wall friction. The model contains isothermal constant area gas flow as a special case, obtained simply by letting the flow rate of the liquid phase equal zero, and hence provides a connection between homogeneous liquid-gas flow and single-component gas flow. Thus it is possible to draw parallels and to view the two-phase flow in the light of known gas dynamics phenomena.

That the mathematical model represents real flow conditions, which is not obvious in the analysis due to the restrictive assumptions necessary, is demonstrated by comparing the theory with results obtained experimentally with homogeneous water-air mixtures.

THE BASIC ASSUMPTIONS

Homogeneous bubbly flow consists of a coarse suspension of gas bubbles in a liquid with a finite-slip velocity between the phases. The bubbles may vary in size but are more or less uniformly distributed; very little is known about the magnitude of the slip velocities. However it is obvious that the phenomenological behavior of the medium will be characterized by the compressibility of the gas phase and the inertia of the dense liquid phase. Furthermore, the thermodynamic properties will be greatly influenced by the thermal state of the liquid.

To obtain a simple model which will account for the compressibility of the gas, the inertia of the liquid, and the

influence of the liquid phase on the thermodynamic properties of the mixture, very restrictive basic assumptions are required (3).

Beside assuming that the mixture is chemically stable and thermodynamically a pure substance, it is also necessary that one considers that: (1) there is no mass transfer between the phases; (2) the liquid phase is incompressible and the gas obeys the perfect gas laws; (3) the phases are locally at the same temperature and pressure (this implies local thermodynamic equilibrium and negligible surface tension); and (4) the flow is continuous to the extent that meaningful mean quantities, such as mixture density and velocity can be defined (this can only be reasonably met when the slip velocity is negligible and the phases are mixed uniformly). Only within this framework of assumptions does it appear possible to develop an analysis and then only for adiabatic or nearly adiabatic boundary conditions. The obvious limitations need to be borne clearly in mind.

PROPERTIES OF THE MEDIUM

It is possible to define the local state of the medium by considering the mass flow rates of the mixture and of the individual phases. For conservation of mass, with homogeneous mixing taking place in unit time, a bulk mixture density can be defined by writing

$$\rho(Q_g + Q_l) = m_g + m_l \quad (1)$$

where

$$m_g = Q_g \rho_g \quad (2)$$

and

$$m_l = Q_l \rho_l \quad (3)$$

It follows that the bulk density of the mixture will be

$$\rho = \left(\frac{\beta}{1 + \beta} \cdot \frac{1}{\rho_g} + \frac{1}{1 + \beta} \cdot \frac{1}{\rho_l} \right)^{-1} \quad (4)$$

where

$$\beta = m_g/m_l \quad (5)$$

is, by definition, the mass flow ratio for the two phases.

Now, if a volume flow ratio is defined as

$$\delta = Q_g/Q_l \quad (6)$$

it also follows from Equations (1) to (3) that

$$\rho/\rho_l = (1 + \beta)/(1 + \delta) \quad (7)$$

Note that for a given pipe flow the mass flow ratio β will be constant; however the bulk density ρ and the volume flow ratio δ will not be constant.

An equation of state for the medium can be obtained by writing the perfect gas equation for the gas phase alone and by transforming it to an equivalent statement with Equation (4) used to eliminate gas density. When this is done it is found that

$$p \left(\frac{1}{\rho} - \frac{1}{1 + \beta} \cdot \frac{1}{\rho_l} \right) = RT \quad (8)$$

where

$$R = \beta R_g/(1 + \beta) \quad (9)$$

Since β and R_g are constant for any given flow, it follows that R will also be constant. In effect Equation (8) may be considered as the equation of state of a pseudo gas which has a specific volume of $1/(1 + \beta)\rho_l$ at infinite pressure.

The specific heats of the medium may be found from the law of mixing. Thus, by considering a time interval of unity

$$C_P = (m_l C_{Pl} + m_g C_{Pg})/(m_l + m_g) = (C_l + \beta C_{Pg})/(1 + \beta) \quad (10)$$

by Equation (5).

Similarly, it is found that

$$C_V = (C_l + \beta C_{Vg})/(1 + \beta) \quad (11)$$

For a typical bubbly water-air flow β is usually of the order of 10^{-2} . Hence the specific heats of the medium are practically equal to the specific heat of the liquid phase. It will be observed that C_P and C_V define R in the same way as in the thermodynamics of gases. That is

$$R = C_P - C_V \quad (12)$$

In fact, Equations (4), (8), (9), (10), and (12) for the pseudo gas all reduce to perfect gas equations as β approaches infinity.

Note, as well, that

$$\gamma = C_P/C_V \quad (13)$$

defines the ratio of specific heats for the pseudo gas in the same way as for a perfect gas. This fact was discovered originally by Tangren et al. (2), who established an adiabatic state path law:

$$p \left(\frac{1}{\rho} - \frac{1}{1 + \beta} \cdot \frac{1}{\rho_l} \right)^\gamma = \text{constant} \quad (14)$$

and showed that

$$\frac{p \left(\frac{\gamma-1}{\gamma} \right)}{T} = \text{constant} \quad (15)$$

Naturally γ is nearly equal to unity for typical homogeneous liquid-gas flows; as a result temperature changes due to pressure variations will be quite small.

The local speed of sound can be found from Equation (14) by evaluating

$$a = \left(\frac{dp}{d\rho} \right)_{\text{adiabatic}}^{1/2}$$

After some algebraic manipulation, there results

$$a = \frac{1 + \delta}{\delta} (\gamma RT)^{1/2} \quad (16)$$

and hence, by using Equations (10), (11), and (12), it is easy to show that the ratio of the speed of sound in the

medium to the speed of sound in gas at the same temperature is

$$\frac{a}{a_g} = \left(\frac{1 + \delta}{\delta} \right) \left[\frac{\gamma \beta}{\gamma_g (1 + \beta)} \right]^{1/2} \quad (17)$$

In other words, the sound speed is much lower.

Woodbury (7) has shown that Equation (16) is physically meaningful insofar as it represents the propagation speed of very weak shock waves.

MACH NUMBER

A concept pertinent to the analysis is that of Mach number, which is defined as the ratio of the bulk velocity of the flow to the local speed of sound, that is

$$N_M = u/a \quad (18)$$

This concept has been used extensively in gas dynamics but appears to be new in the case of two-phase flows. Intuitively, it is reasonable to expect that it will play much the same role in the case of homogeneous bubbly flow as it does in gas dynamics. We will proceed to determine a suitable set of equations by using Mach number and known properties of the medium as independent variables. The validity of the analysis is established in Part II of the paper, which reports the results of our experimental work.

GOVERNING EQUATIONS: ISOTHERMAL BUBBLY PIPE FLOW

So far, the equations obtained are for state properties of the mixture. To proceed further it is necessary to specify the type of flow and to include details of the boundary conditions. It is logical to restrict attention to flow in horizontal pipes of constant cross section and to consider the case of isothermal motion, since unheated bubbly flows are practically at constant temperature. The latter has been discussed by other workers (2, 4, 8), it being argued that irreversible heating due to shear stresses is absorbed by the liquid phase which acts as a constant temperature heat reservoir. Certainly the anticipated change in liquid temperature in most situations is only about 10^{-1}° .

Thus it is assumed that: (1) the flow is steady and one-dimensional; (2) the pipe is of constant cross section, horizontal, and has adiabatic walls; (3) wall friction is the determining factor which causes changes in flow properties; and (4) there are no temperature changes ($dT = 0$).

It then follows from Equations (7) and (8) that

$$\frac{dp}{p} = \frac{1 + \delta}{\delta} \frac{d\rho}{\rho} \quad (19)$$

From consideration of conservation of mass in one-dimensional constant area flow it may be shown that

$$\frac{d\rho}{\rho} = - \frac{du}{u} \quad (20)$$

and by taking a momentum balance (see Appendix 1*) it is found that

$$2 \frac{du}{u} + \frac{dp}{p} \cdot \frac{2\delta}{1 + \delta} \cdot \frac{1}{\gamma N_M^2} = - \frac{4}{D} C_f dx \quad (21)$$

where C_f is a local friction coefficient defined as

$$C_f = \tau_w / \frac{1}{2} \rho u^2$$

* Appendices 1 to 3 have been deposited as Document 9072 with the American Documentation Institute, Photoduplication Service, Library of Congress, Washington 25, D. C., and may be obtained for \$1.25 for photoprints or 35-mm. microfilm.

Additional differential equations can be obtained from the definition of Mach number and the equation for sound speed, Equation (16). From the former it follows that

$$\frac{dN_M}{N_M} = \frac{du}{u} - \frac{da}{a} \quad (22)$$

and from the latter

$$\frac{da}{a} = -\frac{1}{1+\delta} \frac{d\delta}{\delta} \quad (23)$$

where the term on the right-hand side may be restated by differentiating Equation (7) to obtain

$$\frac{d\rho}{\rho} = -\frac{d\delta}{1+\delta} \quad (24)$$

Thus Equation (23) becomes

$$\frac{da}{a} = \frac{1}{\delta} \frac{d\rho}{\rho} \quad (23a)$$

Since wall friction causes changes in flow properties, it is desirable to choose $4C_f dx/D$ as one of the independent variables and to search for solutions in terms of this variable, the Mach number and properties of the medium. On doing so it is found that

$$\frac{du}{u} = \frac{1}{2} \left(\frac{\gamma N_M^2}{1-\gamma N_M^2} \right) \frac{4}{D} C_f dx \quad (25)$$

$$\frac{d\rho}{\rho} = -\frac{1}{2} \left(\frac{\gamma N_M^2}{1-\gamma N_M^2} \right) \frac{4}{D} C_f dx \quad (26)$$

$$\frac{dN_M}{N_M} = \frac{1}{2} \left(\frac{1+\delta}{\delta} \right) \left(\frac{\gamma N_M^2}{1-\gamma N_M^2} \right) \frac{4}{D} C_f dx \quad (27)$$

$$\frac{dp}{p} = -\frac{1}{2} \left(\frac{1+\delta}{\delta} \right) \left(\frac{\gamma N_M^2}{1-\gamma N_M^2} \right) \frac{4}{D} C_f dx \quad (28)$$

One immediately notices the close similarity between these equations and the well-known equations of isothermal constant area gas flow. As in gas dynamics it is seen that the dependent variables change sign on either side of $N_M = \gamma^{-1/2}$. This critical value of the Mach number should then represent the choking limit for a continuous isothermal homogeneous liquid-gas flow. In other words, the velocity of initially supercritical flows should decrease and the velocity of initially subcritical flows increase continuously as long as the Mach number at exit from the pipe does not reach the critical value. As in gas dynamics, when the critical Mach number is reached at the pipe exit, any change in initial conditions tending to increase its value should give rise to new phenomena and the only phenomena likely to occur are a discontinuity (that is a shock, if the flow is initially supercritical) or a breakdown of the homogeneity of the flow. The latter is more likely and is discussed further in Part II.

THE N_M — δ RELATION

It is possible to obtain a parametric relationship between δ and N_M . This relationship may be found by using Equations (20), (23), and (24) to restate Equation (22). The result is

$$\frac{dN_M}{N_M} = \frac{d\delta}{\delta} \quad (29)$$

As in gas dynamics it is convenient to use critical ($N_M = \gamma^{-1/2}$) conditions for reference purposes, it being immaterial whether they actually exist in the flow or not. Thus Equation (29) can be integrated between local and critical limits, which are, respectively

$$N_M = N_M : \delta = \delta$$

and

$$N_M = \gamma^{-1/2} : \delta = \delta^*$$

The outcome is

$$\delta = \gamma^{1/2} \delta^* N_M \quad (30)$$

The physical meaning is clear. For isothermal flow δ varies inversely with p [see Equations (19) and (24)], so that N_M varies inversely with p as well. That is, as pressure drops along the pipe (in subcritical flow) the Mach number and volume flow ratio (air voidage) increase. This is in accordance with physical experience.

WORKING FORMULAS

Useful working formulas may be obtained by using Equation (27) to eliminate $4C_f dx/D$ in Equations (25), (26), and (28) and employing Equation (30). The dependent variables are then found as simple functions of the Mach number and it is possible to integrate between local and critical limits. The results are

$$\frac{u}{u^*} = \frac{1 + \gamma^{1/2} \delta^* N_M}{1 + \delta^*} \quad (31)$$

$$\frac{p}{p^*} = (\gamma^{1/2} N_M)^{-1} \quad (32)$$

and

$$\frac{\rho}{\rho^*} = \frac{1 + \delta^*}{1 + \gamma^{1/2} \delta^* N_M} \quad (33)$$

A friction length formula, which relates the effects of wall friction and pipe length to the state of the substance and Mach number, may also be obtained by using Equations (25), (28), and (30) in Equation (21). In order to integrate the differential equation resulting from this combination, it is necessary to assume a constant average value of the friction coefficient $\bar{C}_f = \int_{x^*}^x C_f dx / (x - x^*)$. The equation then obtained is

$$\begin{aligned} \frac{4}{D} \bar{C}_f (x - x^*) &= 2\delta^* \left(\frac{\gamma^{1/2} N_M - 1}{\gamma^{1/2} N_M} \right) \\ &+ 2 \ln \left(\frac{1 + \delta^*}{1 + \gamma^{1/2} \delta^* N_M} \right) \\ &+ 2\delta^* \ln \left\{ \frac{1 + \gamma^{1/2} \delta^* N_M}{\gamma^{1/2} N_M (1 + \delta^*)} \right\} \quad (34) \end{aligned}$$

This relation gives the length of pipe that will change the Mach number from an initial value N_M to $N_M^* = \gamma^{-1/2}$ at the pipe exit.

GENERAL REMARKS

It has been shown that it is possible to establish a mathematical model of homogeneous two-phase constant area flow which is essentially similar to that for isothermal gas flow and which takes account of known physical phenomena. Naturally the friction coefficient \bar{C}_f will be less tractable than the corresponding coefficient for single-component liquid flows but because it has been possible to deal with gas flow using the idea of a mean coefficient, it is logical to expect that it will also be possible to do so in the present case. Of course, values of \bar{C}_f have to be determined experimentally and thus will take into account deviations from the assumed conditions. In particular experimentally determined values of \bar{C}_f will automatically include variations due to nonuniformity of the velocity profile and finite slip between the phases.

PART II: EXPERIMENTAL INVESTIGATION

EXPERIMENTAL EQUIPMENT AND MEASUREMENTS

A schematic layout of the experimental equipment is shown in Figure 1. The apparatus consisted of a mixing nozzle and test pipe both of which were supported in a horizontal position. Metered water and air were injected separately into the mixing nozzle and then passed into the pipe which had a free discharge to atmosphere. The mixing nozzle was of 4 in. diameter tapering to 1 in. diameter at the exit. The test pipe was coupled directly and consisted of 48 ft. of 1-in. diameter perspex pipe.

It was found by ad hoc experiments that a satisfactory mixture of small air bubbles could be obtained if water was introduced to the mixing nozzle via a number of small high-velocity jets and the water flow rate maintained above 1,000 lb./((sec.)(sq. ft.)). Under such conditions no mechanical device was required to produce mixing, since it was entirely produced by the turbulent conditions in the nozzle itself. The first 6 ft. of the test pipe were used as a calming length to ensure that the experiments were restricted to homogeneous flow in the remaining 42 ft. Static pressure tapings and taps for Pitot probes were provided at 6-ft. intervals downstream of the calming length as shown in Figure 1.

In the course of the experiments, it was found that pressure fluctuations were small except near the exit when critical conditions prevailed and during slugging of the flow. Under all other conditions it was possible to measure pressures and pressure differences to an accuracy of ± 0.15 lb./sq.in. or better. To eliminate inaccuracy of measurement due to water in the connecting tubes the lines were purged with compressed air. The purging techniques were checked by comparing measured pressure drops for single-phase water flow against values obtained with conventional water-mercury manometers. Water and air were metered by calibrated orifice meters and the probable deviations from the true flow rates maintained at $\pm 3\%$ or better throughout the work.

A series of preliminary experiments was carried out on the test pipe for the single-phase flow of air and water separately. Results so obtained were translated into friction factor f_s and Reynolds number N_{Re} . When compared with the universal law of friction in smooth pipes (9),

$$f_s^{-1/2} = 2.0 \log_{10} (N_{Re} f_s^{1/2}) - 0.8 \quad (35)$$

good agreement was obtained.

PRELIMINARY OBSERVATIONS

Flow Regimes

A prerequisite for homogeneous bubbly flow is that the bulk velocity of the mixture be large compared with the rise velocity of small air bubbles. The present experiments showed that a minimum water weight flow rate per unit pipe area of approximately 1,000 lb./((sec.)(sq. ft.)) is required to satisfy this criterion. The value agrees favor-

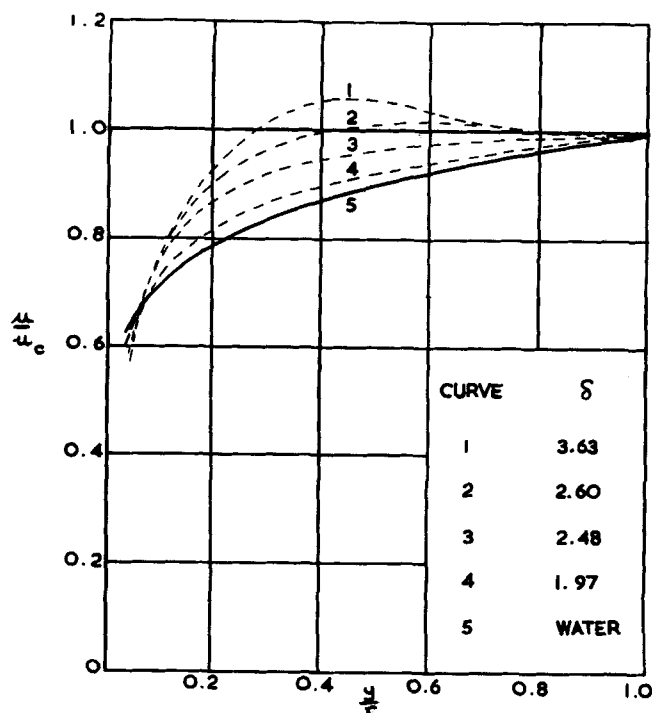


Fig. 2. Effect of volume flow ratio on velocity profile.

ably with that given by James and Silberman (10), who investigated two-phase water-air flow in 2¼- and 4-in. galvanized pipes. Apparently this minimum value applies for all pipes in the range 1 to 4 in. in diameter. Certainly in the present series of experiments it was found homogeneous bubbly flow did not occur when the water flow rate was below 1,000 lb./((sec.)(sq. ft.)) regardless of the value of the volume flow ratio δ . For higher values steady homogeneous bubbly flow was obtained for δ ranging from 0.2 to 3.3. With $\delta < 0.2$ it was found the bubbles concentrated in the upper portion of the pipe. This pattern corresponds with that described by Alves (11), who named it bubble flow as distinct from bubbly flow. With $\delta > 3.3$ it was found the flow became increasingly unsteady and that frothy slugs began to appear.

As will be seen from the above the criteria which define the type of homogeneous bubbly flow considered in Part I were

$$0.2 < \delta < 3.3$$

$$\frac{G_l}{A} > 1,000$$

However, it should be noted that in reality a bubbly type flow of some kind or other will occur over a region considerably wider than is indicated by these limits and that the structure of any given bubbly flow will vary considerably as it proceeds along a pipe. In the experiments the following sequential changes were observed.

The mixture emerged from the nozzle as a coarse suspension of air bubbles. At this point the local volume flow ratio (air voidage) was lowest and the bubbles clearly discernable. The medium was transparent.

As the flow accelerated along the pipe, air voidage increased due to the pressure drop and there was an increase in the homogeneity of the mixture. The medium became more and more opaque until it was no longer possible to distinguish the two phases and it took the appearance of a fine frothy emulsion. It retained these characteristics, subsequently revealed to be characteristics of an essentially uniform velocity profile, until δ just exceeded 3.3 at the exit. As δ became larger a breakdown in homogeneity occurred, the motion first becoming unsteady

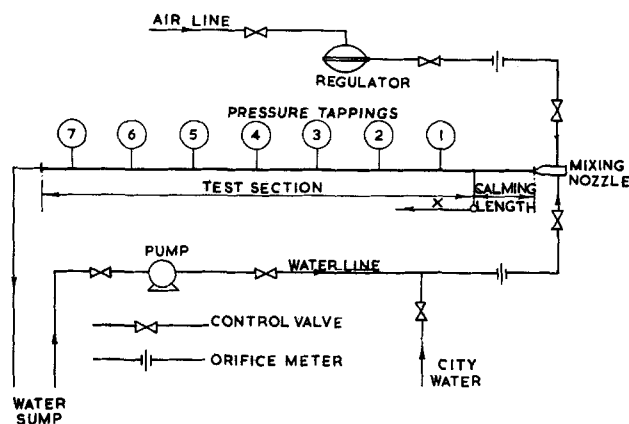


Fig. 1. Schematic flow diagram.

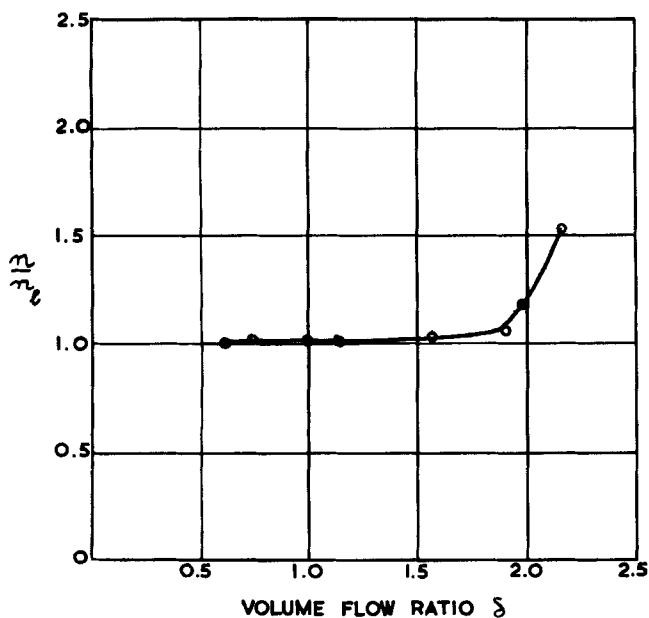


Fig. 3. Effect of volume flow ratio on velocity profile.

and then developing into a frothy slug flow. Very strong slugging occurred when δ was above a value of approximately 15 at the pipe inlet.

Velocity Profiles

Velocity profiles of the two-phase flow for different values of volume flow ratio are shown in Figure 2. These profiles were obtained by traversing along the horizontal radius and are representative of results obtained at all test sections along the pipe. For comparison the velocity profile for single-component water flow at the superficial water flow rate (that is, the flow rate of the water phase alone) is also shown.

TABLE 1. SUMMARY OF EXPERIMENTS

Run No.	G_t , lb./sec.	β	T , °R.	Flow conditions	Mach No. at exit	Volume flow ratio at exit
1	8.05	$\frac{1}{1,480}$	532	Subcritical	0.54	0.57
2	7.30	$\frac{1}{760}$	532	Subcritical	0.69	1.11
3	6.68	$\frac{1}{540}$	532	Subcritical	0.74	1.55
4	6.24	$\frac{1}{340}$	532	Subcritical	0.88	2.48
5	6.24	$\frac{1}{252}$	533	Choked at exit	1.0	3.4
6	5.90	$\frac{1}{231}$	532	Choked	1.0	3.6
7	5.55	$\frac{1}{195}$	534	Choked		
8	4.92	$\frac{1}{165}$	532	Choked		

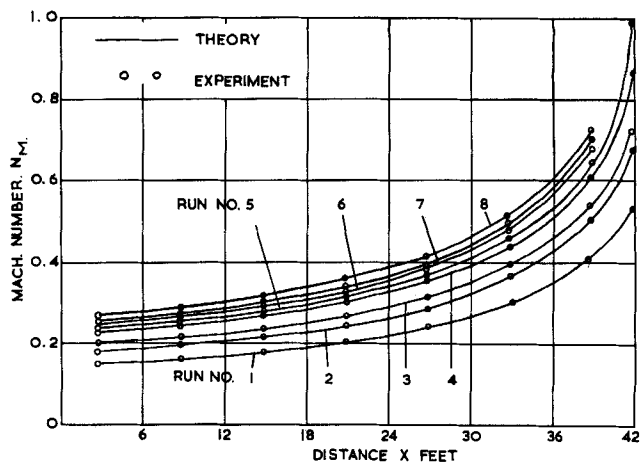


Fig. 4. Variation of Mach number along pipe.

The experiments showed that for a given superficial water flow rate, the two-phase profile is a function of volume flow ratio δ alone. With small values of δ the velocity profile was essentially the same as for water. This was established by determining expressions for velocity profiles in the form

$$\frac{u}{u_c} = (y/r)^{1/n} \quad (36)$$

and by comparing values of n with $n = n_1$ for the superficial water flow. The results are shown in Figure 3. As will be seen the two-phase profiles were similar to those of the superficial water flow for δ less than 1.5. It will be observed from Figure 2 that variation in profile shape was small for values of δ up to about 2. However further increase in voidage gave rise to a rapid change in profile shape, the profile becoming fuller. Humping of the profile occurred when δ was about 3.

VARIATION OF FLOW PROPERTIES

Eight separate experiments were carried out for different mass flow ratios and water flow rates. The test conditions are summarized in Table 1.

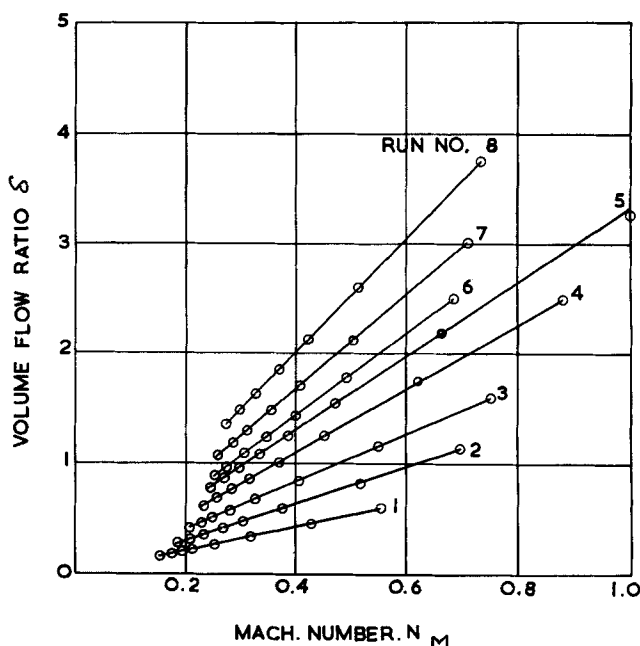


Fig. 5. Mach number against volume flow ratio.

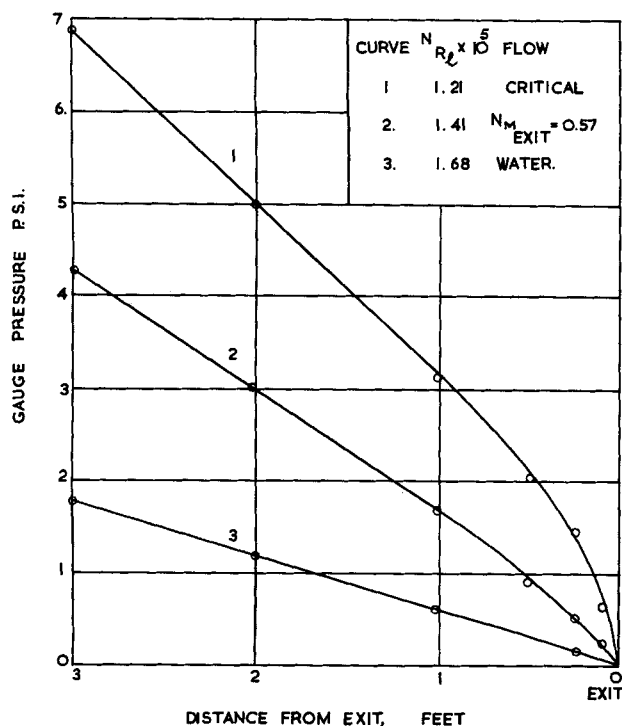


Fig. 6. Pressure drop near exit.

Now, for a fixed value of β , providing the static pressure is known, it is possible to compute the volume flow ratio (by using the equation of state for perfect gases) and also to find the sound speed. Accordingly, in each experiment values of static pressure were determined along the pipe. Mean values of flow velocity were obtained from Pitot readings by taking the dynamic pressure to be $\rho u^2/2$. The results were then used to evaluate Mach numbers. Values of Mach numbers so found are shown in Figure 4. Figure 5 shows the relationship between volume flow ratio and Mach number for the eight experiments. As predicted by theory there is a linear relationship in each case. The theoretical curves shown in Figure 4 were obtained for runs 5 to 8 (choked at exit) by using Equation (32) of the theoretical analysis, namely

$$\frac{p}{p^*} = (\gamma^{1/2} N_M)^{-1} \quad (37)$$

to evaluate the Mach numbers. Corresponding curves for runs 1 to 4 (subcritical) were obtained by extrapolating to find the critical volume flow ratio (using Figure 5) and employing Equation (30) of the analysis, namely

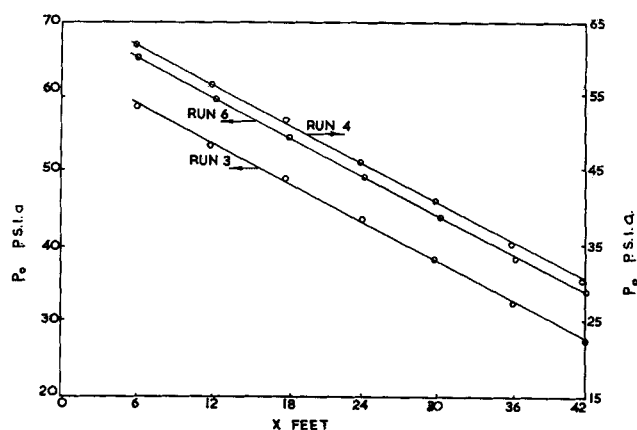


Fig. 8. Measured stagnation pressures.

$$\frac{\delta}{\delta^*} = \gamma^{1/2} N_M \quad (38)$$

So far as flow properties are concerned the theory appears to represent real flow conditions adequately.

CRITERION FOR CHOKING

It will be observed from Figure 4 that the change in Mach number was rapid as the flow conditions became critical. Similar tendencies are reflected in Figure 6 where the measured pressure distribution over the last 3 ft. of the pipe are shown for a choked bubbly flow, a bubbly flow with subcritical exit, and for single-phase flow of water. Experiments confirmed that once critical conditions had been reached at exit, further increase of the mass flow ratio by varying upstream conditions gave rise to the appearance of frothy slugs which moved upstream as the mass flow ratio was increased. The breakdown occurred at a volume flow ratio of approximately 3.3. An exact value could not be determined due to unsteadiness. Nevertheless the evidence was sufficient to establish adequacy of $N_M^* = \gamma^{-1/2}$ as a choking limit and to indicate that the transition from bubbly flow to bubbly slug flow can probably be explained in terms of the humping of the velocity profile. The need of further detailed study is obvious.

FRICTION FACTOR

For the theory of Part I to be useful it is necessary that values of the mean friction coefficient be known and, bearing in mind the assumptions made, it is clear that one must determine the values experimentally. It was found that values of local friction coefficient could be deter-

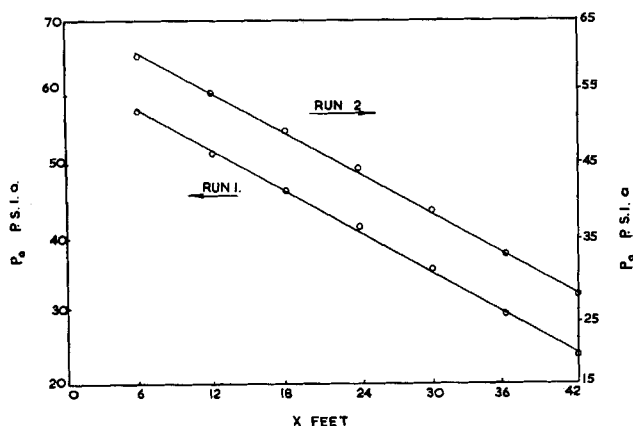


Fig. 7. Measured stagnation pressures.

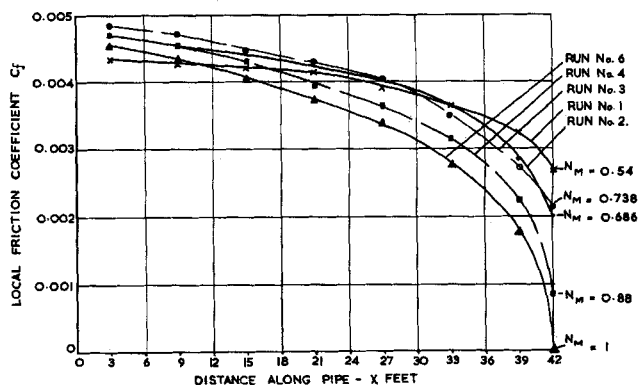


Fig. 9. Values of local friction coefficient.

TABLE 2. AVERAGE FRICTION COEFFICIENT

Run No.	β	Conditions at inlet to test section				Conditions at pipe exit				Average value of \bar{C}_f	Estimated value of \bar{C}_f
		δ	\bar{u} , ft./sec.	a , ft./sec.	N_m	δ	$\bar{\mu}$	a	N_m		
1	$\frac{1}{1,480}$	0.155	27.4	185	0.148	0.566	37.1	68.7	0.54	0.0039	0.0039
2	$\frac{1}{760}$	0.289	27.8	155	0.179	1.11	45.5	66.2	0.686	0.0041	0.0040
3	$\frac{1}{540}$	0.415	27.9	140	0.199	1.55	49.8	67.5	0.738	0.0041	0.0041
4	$\frac{1}{340}$	0.629	30.0	135	0.223	2.48	64.2	73	0.878	0.0039	0.0041
6	$\frac{1}{231}$	0.885	32.7	134	0.244	3.6	80.3	80.3	1.0	0.0037	0.0042

mined simply by measuring the static and stagnation pressures in addition to the flow velocity. (As before the density was taken to be the density of the liquid phase and slip neglected.)

A series of five experiments was conducted, corresponding with runs 1 to 4 and 6 in which the stagnation pressure was measured directly at 6-ft. intervals along the pipe. Measurements were made at the radius where the velocity was equal to the average velocity for the cross section. The results are shown in Figures 7 and 8. As will be observed, the stagnation pressure varied linearly along the pipe.

To evaluate the local friction coefficient, the momentum equation, Equation (21), was put into the form (see Appendix 2):

$$C_f = \frac{(dp_o/dx)}{\frac{2}{D} \left(\frac{1+\delta}{\delta} \right) \gamma p N_M^2 \left\{ \frac{\gamma N_M^2 - 2}{2(1 - \gamma N_M^2)} \right\}} \quad (39)$$

Values of C_f determined with Equation (39) are shown in Figure 9. Average values of \bar{C}_f obtained by graphical integration are given in Table 2.

The results show that it is possible to establish values of \bar{C}_f which can be fed into the theory for the purpose of predicting pressure drop. Furthermore \bar{C}_f is seen to be relatively insensitive to Mach number. This is not unexpected as mean friction coefficients for subsonic gas flow are also known to be insensitive to Mach number.

To cast further light on friction, a number of high-speed motion pictures were taken of the flow immediately adjacent to the pipe wall. The photographs showed that with the exception of an occasional bubble that migrated into the friction layer and almost immediately returned to the mainstream, the friction layer contained only water. In other words the bubbly flow was surrounded by an annular water film.

In view of this information, thought was given to the likelihood of predicting friction coefficients from pipe flow data, as is done for subsonic gas flows. Knowing the shear stress would be determined by the viscosity of water in the friction layer and by the inertia of the bubbly flow, we believed the logical dimensionless variable to be

$$N_B = \frac{D\bar{u}}{\nu_l} \left(\frac{1+\beta}{1+\delta} \right) \quad (40)$$

This dimensionless group is a particularly fortunate one,

because any given flow has only one value of N_B (see Appendix 3).

Estimated values of \bar{C}_f obtained by calculating N_B and by using data for single-component flow in smooth wall pipes are shown in Table 2. The values are sufficiently close for most practical purposes. However there is need of additional experimental work to verify that the approach can be used generally.

CONCLUSION

From the foregoing it is possible to conclude that the mathematical model of isothermal homogeneous two-phase flow derived in Part I is realistic and is directly applicable if values of mean friction coefficient are available. The Mach number has been shown to be a meaningful variable, in terms of which the volume flow ratio and friction coefficient can be rationalized. In particular $N_M^* = \gamma^{-1/2}$ is established as the choking limit for homogeneous flow and it is seen that the breakdown to slug flow is somehow due to humping of the velocity profile. The criteria for the occurrence of homogeneous bubbly flow in a 1-in. pipe are found to be liquid flow rate greater than 1,000 lb./ (sec.) (sq. ft.) with values of volume flow ratio between 0.2 and 3.3.

NOTATION

A	= cross-sectional area of pipe
a	= speed of sound
C_f	= local friction coefficient
\bar{C}_f	= mean friction coefficient
C_l	= specific heat of liquid phase
C_P	= specific heat at constant pressure
C_V	= specific heat at constant volume
D	= diameter of pipe
f_s	= single-phase friction factor [see Equation (35)]
G	= weight flow rate
m	= mass flow rate
N_B	= similarity parameter for bubbly flow
N_M	= Mach number
N_{Re}	= Reynolds number
n	= index in Equation (36)
p	= static pressure, abs.
p_o	= stagnation pressure
Q	= volume flow rate
r	= pipe radius
R	= constant in equation of state
T	= static temperature, abs.

u = velocity
 u_c = velocity at center of pipe
 \bar{u} = average velocity
 x = distance along pipe
 y = distance from pipe wall

Greek Letters

β = mass flow ratio
 δ = volume flow ratio
 γ = ratio of specific heats
 ν = kinematic viscosity
 ρ = density
 τ_w = wall shear stress
 μ = dynamic viscosity

Subscripts

g = gas phase
 l = liquid phase

Superscript

* = critical conditions for which $N_M = \gamma^{-1/2}$

LITERATURE CITED

1. Mottard, E. J., and C. J. Shoemaker, *Natl. Aeronaut. Space Admin. Tech. Note D-991* (1961).
2. Tangren, R. F., C. H. Dodge, and H. S. Seifert, *J. Appl. Phys.*, **20**, No. 7, 637-645 (1949).
3. Muir, J. F., and R. Eichhorn, *Proc. Heat Trans. Fluid Mech. Inst., Stanford*, 183-204 (1963).
4. Campbell, I. J., and A. S. Pitcher, *Proc. Roy. Soc. London*, **243A**, 534-545 (1957).
5. Zuber, N., *J. Heat Transfer*, **82C**, 255-258 (1960).
6. Levy, S., *J. Heat Transfer*, **85C**, 137-152 (1963).
7. Woodbury, S. P., M.E. thesis, Univ. New South Wales, in preparation.
8. Hsieh, D. Y., and M. S. Plesset, *Phys. Fluids*, **4**, No. 8, 970-975 (1961).
9. Schlichting, H., "Boundary Layer Theory," 4 ed., McGraw-Hill, New York.
10. James, W., and E. Silberman, *St. Anthony Falls Hydraulic Lab. Tech. Paper No. 26*, Ser. B, Univ. Minnesota.
11. Alves, G. E., *Chem. Eng. Progr.*, **50**, No. 9, 449-459 (1954).

Manuscript received March 2, 1966; revision received June 17, 1966; paper accepted June 22, 1966.

Stability of a Fluid in a Rectangular Region Heated from Below

MICHAEL R. SAMUELS and STUART W. CHURCHILL

University of Michigan, Ann Arbor, Michigan

Finite-difference methods were used to compute hydrodynamic instability due to natural convection in an enclosed horizontal rectangular region heated from below. Critical Rayleigh numbers were determined for a series of Prandtl numbers and length-to-height ratios. For Prandtl numbers greater than unity excellent agreement was obtained between these calculations and the values predicted by Kurzweg on the basis of a linearized theory. However, for Prandtl numbers less than unity the critical Rayleigh numbers exhibited a dependence on N_{Pr} , which was not predicted by the linearized theory. For Rayleigh numbers greater than the critical, complete temperature and velocity fields were determined.

The calculations assumed that the fluid motion is two dimensional. Experiments have indicated that the flow may be two or three dimensional depending on minor perturbations in the boundary conditions.

Although a number of metastable two-dimensional circulations are possible for symmetrical initial conditions, the calculation always converged to a single, unique solution for any asymmetric initial condition.

Situations in which a small perturbation can cause complete rearrangement of the system are termed *unstable*. Such situations are of special interest to engineers, since an instability may pose difficulties in design and operation.

Natural convection can be described by the equations of conservation of mass, energy, and momentum. Analytical solutions for these coupled, partial differential equations are difficult, if not impossible, to obtain except for

very idealized cases. However, the use of finite-difference techniques has led to solutions for a number of important problems (1, 2, 6, 19).

The objective of this work was to demonstrate the usefulness of finite-difference techniques in the study and characterization of unstable systems. In particular, instability due to natural convection in an enclosed, horizontal region of rectangular cross section heated from below was studied.